

# The critical role of snowmelt onset-driven vapor pressure deficit variations in wildfire dynamics of northern latitudes

Downloaded from: https://research.chalmers.se, 2025-11-15 10:15 UTC

Citation for the original published paper (version of record):

Xu, H., Chen, H., Chen, D. et al (2025). The critical role of snowmelt onset-driven vapor pressure deficit variations in wildfire

dynamics of northern latitudes. Earth's Future, 13(10). http://dx.doi.org/10.1029/2025EF006367

N.B. When citing this work, cite the original published paper.

research.chalmers.se offers the possibility of retrieving research publications produced at Chalmers University of Technology. It covers all kind of research output: articles, dissertations, conference papers, reports etc. since 2004. research.chalmers.se is administrated and maintained by Chalmers Library



# **Earth's Future**



# RESEARCH ARTICLE

10.1029/2025EF006367

#### **Key Points:**

- Shifts in snowmelt onset critically influence the incidence of wildfires primarily through regulating vapor pressure deficit dynamics
- Vapor pressure deficit is geographically pronounced in 47.5% of the areas, contributing 57.1% of the influencing role
- The influencing role through vapor pressure deficit is doubled the contribution from plant water deficit or fuel moisture and availability

#### **Supporting Information:**

Supporting Information may be found in the online version of this article.

#### Correspondence to:

B. He, hebin@bnu.edu.cn

### Citation:

Xu, H., Chen, H. W., Chen, D., Xiao, C., Xiao, J., He, B., et al. (2025). The critical role of snowmelt onset-driven vapor pressure deficit variations in wildfire dynamics of northern latitudes. *Earth's Future*, *13*, e2025EF006367. https://doi.org/10.1029/2025EF006367

Received 27 MAR 2025 Accepted 16 SEP 2025

# **Author Contributions: Conceptualization:** Bin He

Formal analysis: Hongtao Xu
Funding acquisition: Deliang Chen,
Jingfeng Xiao, Lanlan Guo
Investigation: Hongtao Xu, Cunde Xiao
Methodology: Hongtao Xu, Hans
W. Chen, Bin He
Software: Hongtao Xu, Deliang Chen,
Cunde Xiao, Jingfeng Xiao, Aifeng Lv,
Lanlan Guo, Wenping Yuan,
Yongshuo Fu, Xingming Hao,
Ziqian Zhong, Ling Huang, Tiewei Li,
Rui Tang, Xiangqi He, Xinrui Guo,
Yang Chu

Writing - original draft: Hongtao Xu

#### © 2025. The Author(s).

This is an open access article under the terms of the Creative Commons
Attribution-NonCommercial-NoDerivs
License, which permits use and
distribution in any medium, provided the original work is properly cited, the use is non-commercial and no modifications or adaptations are made.

# The Critical Role of Snowmelt Onset-Driven Vapor Pressure Deficit Variations in Wildfire Dynamics of Northern Latitudes

Hongtao Xu<sup>1,2</sup> , Hans W. Chen<sup>3</sup> , Deliang Chen<sup>4</sup> , Cunde Xiao<sup>1</sup> , Jingfeng Xiao<sup>5</sup> , Bin He<sup>1,6</sup> , Aifeng Lv<sup>7</sup>, Lanlan Guo<sup>1</sup> , Wenping Yuan<sup>8</sup> , Yongshuo Fu<sup>9</sup>, Xingming Hao<sup>10</sup> , Ziqian Zhong<sup>3</sup> , Ling Huang<sup>11</sup>, Tiewei Li<sup>1</sup> , Rui Tang<sup>1</sup>, Xiangqi He<sup>1</sup>, Xinrui Guo<sup>1</sup>, and Yang Chu<sup>1</sup>

<sup>1</sup>State Key Laboratory of Earth Surface Processes and Disaster Risk Reduction, Faculty of Geographical Science, Beijing Normal University, Beijing, China, <sup>2</sup>College of Geography and Environmental Sciences, Zhejiang Normal University, Jinghua, China, <sup>3</sup>Department of Space, Earth and Environment, Division of Geoscience and Remote Sensing, Chalmers University of Technology, Gothenburg, Sweden, <sup>4</sup>Department of Earth System Sciences, Tsinghua University, Beijing, China, <sup>5</sup>Earth Systems Research Center, Institute for the Study of Earth, Oceans, and Space, University of New Hampshire, Durham, NH, USA, <sup>6</sup>Akesu National Station of Observation and Research for Oasis Agro-Ecosystem, Xinjiang, China, <sup>7</sup>Key Laboratory of Water Cycle and Related Land Surface Processes, Institute of Geographic Sciences and Natural Resources Research, Chinese Academy of Sciences, Beijing, China, <sup>8</sup>Institute of Carbon Neutrality, Sino-French Institute for Earth System Science College of Urban and Environmental Sciences, Peking University, Beijing, China, <sup>9</sup>College of Water Sciences, Beijing Normal University, Beijing, China, <sup>10</sup>State Key Laboratory of Desert and Oasis Ecology, Xinjiang Institute of Ecology and Geography, Chinese Academy of Sciences, Urumqi, China, <sup>11</sup>College of Urban and Environmental Sciences, Peking University, Beijing, China

**Abstract** Interannual variability in snowmelt onset triggers dynamic responses in processes like surface energy exchange and the hydrological cycle through interactions between vegetation, soil and atmosphere, significantly affecting subsequent fire weather. However, it still remains unclear how shifts in snowmelt onset regulate fire weather and thereby wildfire dynamics during the following seasons. We analyze snowmelt onset dates and wildfire data for northern latitudes (>40°N) and find that interannual variability in snowmelt onset critically influences wildfire dynamics during post-snowmelt periods, with earlier snowmelt tending to increase wildfire incidence. This influencing role is primarily associated with the snowmelt onset-induced variations in vapor pressure deficit, which is geographically pronounced in 47.5% of the northern latitudes, contributing 57.1% of the total influencing role, approximately doubling the contribution from plant water deficit or fuel moisture content and fuel availability. Mechanistically, compared to late snowmelt onset, early vegetation spring green-up caused by an earlier occurrence in snowmelt leads to early moisture consumption. This, in turn, amplifies plant water deficits, which limit evaporative cooling and increase sensible heat fluxes, exacerbating atmospheric dryness and creating favorable conditions for wildfires during the post-snowmelt period. The reveal of these mechanisms has important implications for assessing wildfire risk, enhancing wildfire simulations and forecasting in regions vulnerable to ongoing and future climate change, and projecting carbonclimate feedback.

Plain Language Summary Shifts in snowmelt onset trigger dynamic responses of biophysical and biogeochemical processes, which are important in shaping vegetation dynamics and fire weather, and ultimately affect wildfire dynamics. We used multi-source data to examine the relationship between snowmelt onset and wildfire dynamics. Our study found that shifts in snowmelt onset critically influence wildfire dynamics, with an earlier snowmelt onset tending to increase wildfire incidence. This influencing role is primarily through variations in vapor pressure deficit induced by shifts in snowmelt onset, which is observed in 47.5% of the regions and contributed 57.1% of the total influencing role. Further mechanistic analysis showed that, compared to late snowmelt, earlier occurrence in snowmelt triggers early vegetation green-up, leading to premature moisture consumption and intensifying plant water deficits. This reduction in moisture limits evaporative cooling and boosts sensible heat fluxes, thereby increasing atmospheric dryness. Such conditions foster a conducive environment for wildfires after snowmelt. Our results have significant implications for wildfire risk assessment, and enhancing wildfire simulations and forecasting in snow-covered regions.

Writing – review & editing: Hans W. Chen, Deliang Chen, Cunde Xiao, Jingfeng Xiao, Bin He, Aifeng Lv, Lanlan Guo, Wenping Yuan, Yongshuo Fu, Xingming Hao, Ziqian Zhong, Ling Huang, Tiewei Li, Rui Tang, Xiangqi He, Xinrui Guo

#### 1. Introduction

In the past two decades, the increasing occurrence of wildfires in the northern mid-to-high latitudes has exerted extensive impacts on ecosystem function and the global terrestrial carbon cycle (Zheng et al., 2023). Shifts in ignition patterns (Goulden et al., 2017; Pausas & Keeley, 2021), dry fuels (Flannigan et al., 2005, 2016), and especially favorable fire weather conditions (Rantanen et al., 2022; Scholten et al., 2022; Westerling et al., 2006; Zheng et al., 2021), aused by anthropogenic warming have been widely acknowledged as the key drivers of the increase in wildfire frequency and intensity. However, due to the unique presence of snow cover in cold regions (Koshkin et al., 2022; Li et al., 2017), anthropogenic warming has also triggered changes in snowmelt onset, which may further regulate fire weather and influence wildfire dynamics during the following seasons (Goulden et al., 2017; Zona et al., 2022). Given the increasing role of fire carbon emissions in the global carbon cycle, it is imperative to assess the impact of changes in earlier snowmelt on wildfire dynamics.

Snow is an important component of global biophysical and biogeochemical processes (Ban et al., 2023; Jakobs, 2021; Light et al., 2022; Milly & Dunne, 2020; Vrese et al., 2021), particularly in high altitude and latitude regions. Crucially, the onset of snowmelt controls the start time of meltwater entry into biophysical and biogeochemical processes, which in turn plays a vital role in shaping ecosystem functioning and the climate at both local and global scales (Ban et al., 2023; Fontrodona-Bach et al., 2023; Vavrus, 2007; Vrese et al., 2021). For instance, increasing temperatures in early spring trigger earlier occurrence in snowmelt and vegetation green-up, leading to early consumption of soil moisture. This consequently leads to amplified atmospheric warming and drought in the following seasons (Lian et al., 2020). Additionally, atmospheric warming creates favorable conditions for the development of thunderstorms and lightning (Chen et al., 2021), which increases the likelihood of dry fuel ignition. Although a few regional or local studies have linked wildfire activities to interannual variability in snowmelt onset dates (Scholten et al., 2022; Westerling et al., 2006), the primary process and the underlying mechanism by which shifts in snowmelt onset dates influences wildfire dynamics remains unclear.

Here, we find that interannual variability in snowmelt critically influences wildfire dynamics during post-snowmelt periods, with earlier snowmelt tending to increase wildfire incidence. This influencing role was primarily through snowmelt onset-induced variations in vapor pressure deficit (VPD). To examine the influence of earlier snowmelt on subsequent wildfire dynamics, we firstly analyzed the dynamics of snowmelt onset extracted from multiple snow water equivalent (SWE) and brightness temperature data sets, and investigated its relationship with the number of wildfire events and burned area based on satellite-derived observations. To investigate the underlying mechanisms of this relationship, we examined the linkage between snowmelt dates and wildfire dynamics considering possible intermediate variables including fire weather, burning conditions, and fuel moisture content and potential fuel availability.

#### 2. Materials and Methods

#### 2.1. Materials

### 2.1.1. Burned Area and Number of Wildfire Events

The MODIS sensors onboard the Terra and Aqua platforms play a significant role in monitoring wildfires and are a crucial source of global data on the locations of wildfires and burned areas (Giglio et al., 2010). In this study, we obtained the monthly global burned area at a spatial resolution of 500 m during 2001–2022 from the MCD64A1 data set. The MCD64A1 burned area mapping approach combines 500 m MODIS surface reflectance imagery with 1 km MODIS active wildfire observations, which enables accurate and detailed mapping of burned areas (Giglio et al., 2015). To make a robust estimate, we used only the monthly burned area data with sufficient valid data, as determined by the valid data flag—a quality assurance indicator (Qin et al., 2019). The valid data flag assesses data availability for burned area mapping, with "sufficient valid data" indicating that the reflectance time series within the 500 m grid cell contained adequate high-quality observations for reliable burned area monitoring (Giglio et al., 2015). The information on the number of wildfire events for 2001–2022 was derived from the MCD14DL data set. The number of wildfire events products were generated using automated wildfire detection techniques to generate the daily global number of wildfire events information within each 1 × 1 km grid cell, including essential details such as the geographic coordinates, date, and time of wildfires and confidence coefficients. To obtain robust estimates, we focused on the wildfires with a confidence coefficient threshold of 50%

XU ET AL. 2 of 16

23284277, 2025, 10, Downle

or higher (Giglio et al., 2016). To match the spatiotemporal resolution of the other data, the burned area and number of wildfire events were aggregated and summed within each  $0.25 \times 0.25^{\circ}$  grid cell at the monthly scale.

### 2.1.2. Climate and Other Auxiliary Data

The monthly climate data from 2001 to 2022, including soil moisture, precipitation, and air temperature, evapotranspiration, potential evapotranspiration, sensible heat, surface albedo, downward radiation, net radiation data, were derived from the fifth-generation European Center for Medium-Range Weather Forecasts (ECMWF) reanalysis of land variables (ERA5-Land) data set with a spatial resolution of 0.1 × 0.1° (Muñoz-Sabater et al., 2021). The vapor pressure deficit (VPD) was calculated using 2 m air temperature, dew point temperature, and altitude following the method outlined by Yao et al. (2023). The monthly climatic water deficit (CWD) (i.e., the difference between the potential evapotranspiration and actual evapotranspiration) from 2001 to 2022 was derived from the TerraClimate data set with a 1/24° resolution (Abatzoglou, Balch, et al., 2018; Abatzoglou, Dobrowski, et al., 2018). The fuel moisture content and potential fuel availability from 2001 to 2022 was assessed using the buildup index (BUI). These data were obtained from historical fire danger indices provided by the Copernicus Emergency Management Service for the European Forest Fire Information System (EFFIS). This data set includes daily 0.25° fire danger indices based on three models developed in Canada, the US, and Australia (Kropp et al., 2022). The BUI is a critical component of the Fire Weather Index System and is a measure of weighted duff moisture code and drought code, indicating overall fuel moisture content and potential fuel availability for combustion. The climate and auxiliary data were aggregated and averaged within each  $0.25 \times 0.25^{\circ}$  grid at the monthly scale. The solar-induced chlorophyll fluorescence-based gross primary productivity (GPP) product was obtained from Li and Xiao (2019), which provided 8-day GPP estimates spanning from 2000 to 2022 at a spatial resolution of 0.05°. To harmonize with the temporal resolutions of other climate data sets, we aggregated the 8-day GPP estimates into a monthly average. The start of growing season was derived from MCD12Q2 data set, which provided annual phenology estimates since 2001 at a spatial resolution of 500 m (Friedl et al., 2019). The aridity index data set was obtained from Zomer et al. (2022), and was calculated based on the ratio of multi-yearly average precipitation between 2001 and 2022 to potential evapotranspiration. Additionally, to align with the spatial resolutions among multiple data sets, we unified and averaging aggregated the spatial resolution to 0.25°.

#### 2.2. Methods

### 2.2.1. Extraction of Snowmelt Onset

We determined the snowmelt onset dates from the snow water equivalent and brightness temperature (Tb; Maslanik & Stroeve, 2004) data sets, separately (Figure S1 in Supporting Information S1). For the SWE-based snowmelt onset, we defined the snowmelt onset as the last day of the peak SWE during the snow year (i.e., 1 September to 31 August; Inouye & McGuire, 1991; Kropp et al., 2022). Low SWE values can make it difficult to accurately measure and characterize the melting process. Consequently, we excluded pixels with maximum SWE values of <40 mm (Fontrodona-Bach et al., 2023; Kropp et al., 2022). To eliminate locations with no persistent snow cover or snowmelt timing, we also excluded pixels with <30 days of SWE observations above the minimum threshold of 40 mm during the spring (February-June; Kropp et al., 2022). We used the daily SWE data from the ERA5-Land (Muñoz-Sabater et al., 2021) and GLDAS 2.2 (Li et al., 2019) data sets to determine the timing of the onset of snowmelt. In addition, snowmelt (i.e., the transition from dry snow to a wet regime) can also be recognized using the sharp change in the difference in the Tb (TbD = Tb (19V) – Tb (37V)), which is calculated as the difference of the brightness temperature between the vertical polarization of 19 (SSMI and SSMIS) or 18 (SMMR) GHz and 37 GHz from passive microwave sensors (Takala et al., 2009; Wang et al., 2013). To increase the robustness of our calculations, we also calculated the onset of snowmelt using the daily Tb extracted from the SMMR, SSM/I, and SSMIS. The onset of snowmelt was defined as the day when the difference in the daily TbD and the previous 3-day average (M) was greater than a threshold (TH1 =  $0.35 \times M$ ) for four or more consecutive days (Wang et al., 2013). Given the predominant occurrence of snowmelt during spring months, we reported snowmelt onset dates using the day of the calendar year (January-December) in this study to enable robust analysis of its cascading effects on wildfire activity throughout the primary fire season (March-October; Figure S2 in Supporting Information S1).

XU ET AL. 3 of 16

## 2.2.2. Quantifying the Influence of Earlier Snowmelt Onset on Subsequent Wildfires

We used partial correlation analysis to investigate the relationship between the onset of snowmelt and the number of wildfire events and burned area during the post-snowmelt period after removing the effects of temperature and total precipitation. To explore how the earlier snowmelt onset affected the number of wildfire events and burned area during the post-snowmelt period, we investigated the influence of snowpack on vegetation growth and climate (Ban et al., 2023; Inouye & McGuire, 1991; Pirk et al., 2023; Vavrus, 2007; Vrese et al., 2021; Zona et al., 2022), as well as other factors influencing the occurrence of wildfires (Jones, et al., 2022; Pausas & Keeley, 2021; Zheng et al., 2023), by considering three main pathways: fire weather, vegetation dryness, and fuel moisture content and fuel availability for combustion. The fire weather, vegetation dryness, and fuel moisture content and fuel availability for combustion were denoted by the average VPD, CWD, and BUI, respectively. We conducted partial correlation analyses between the snowmelt onset dates and the VPD, CWD, and BUI after removing the effects of temperature and total precipitation. Similarly, to explore the effectiveness of each pathway on the number of wildfire events and burned area during the post-snowmelt period, we also conducted partial correlation analyses between VPD, CWD, and BUI and the number of wildfire events and burned area. To minimize the influence of deliberate ignition, we analyzed only those pixels that were covered with natural vegetation before the wildfire based on the annual land-cover type data provided by the ESA Climate Change Initiative (ESA, 2017). This approach meant that we excluded pixels associated with fires on farmlands, wetlands, urban and built-up land, and other land types with minimal vegetation. Considering the main fire season typically started in March and ended in October (Figure S2 in Supporting Information S1), and the burned area and number of wildfire events during this period accounted for 98.5% and 97.1% of the annual totals, respectively (Figure S2 in Supporting Information S1). Therefore, this study defined the post-snowmelt period as the duration from the month following snowmelt onset to October. The average values of the VPD, CWD, BUI, and temperature during the post-snowmelt period were calculated, and the cumulative values of the precipitation, number of wildfire events and burned area were calculated. Considering the climatic variables are coupled, direct analysis of the relationship between snowmelt onset and climatic variables will cause greater uncertainty in the results. To reduce the influence of the long-term dependencies of these variables, each variable was calculated as the year-to-year variations. In terms of each variable, the year-to-year variation in this study was calculated based on two consecutive years, which were estimated as the value of the following year minus the previous year. Different from the long-term trend of snowmelt onset shown in Figure 1, such an approach based on the difference between consecutive years effectively isolates short-term variability by mathematically decoupling the signal from potential confounding effects of long-term covariate dependencies (Forzieri et al., 2020; Lai et al., 2024). We only focused on the pixels in which for any two consecutive years, a wildfire occurred in at least 1 year. To increase the sample size and enhance the reliability, the partial analyses were conducted using all burned pixels within a  $9 \times 9$ pixel moving window. To further quantify the influence of earlier snowmelt onset on the dynamics of postsnowmelt wildfires through the three pathways, we conducted a path analysis to explore the underlying mechanisms associated with the linkage between the onset of snowmelt and the number of wildfire events and burned area during the post-snowmelt period using a structural equation model (SEM). The SEM also considered the influences of precipitation and temperature on VPD, CWD, BUI, number of wildfire events, and burned area. The SEM was applied at the grid level and was based on the normalized year-to-year variations. The path effect through each pathway (e.g., VPD) was the indirect path effect of the snowmelt onset on the number of wildfire events (burned area) during the post-snowmelt period via VPD. This indirect path effect was estimated as the product of the two direct path effects: (a) snowmelt onset on VPD, and (b) snowmelt onset-induced VPD on the number of wildfire events (burned area). We estimated the path effect for each pathway and then used the value to represent the magnitude and direction of the impact. We used the adjusted goodness of fit (AGFI), the Tucker-Lewis index (TLI), the Chi-square P value for the model, and the ratio of chi-square to the degrees of freedom ( $\gamma^2/df$ ) to verify the effectiveness of the constructed SEM. The constructed SEM was accepted when the following conditions were met: AGFI > 0.9, TLI > 0.95, P > 0.05, and  $\gamma^2/df < 3$  (Hu & Bentler, 2009; Semain, 2015; Zheng & Bentler, 2024). It should be noted that the Chi-square P value assesses the overall fit and the discrepancy between the true and fitted covariance matrices, and a P value greater than 0.05 indicates no significant differences between the true and fitted covariance matrices, suggesting that the SEM provides a good fit of data. As with the partial correlation analysis, the path analysis was conducted using  $7 \times 7$ ,  $9 \times 9$ , and  $11 \times 11$ pixels spatial moving windows.

XU ET AL. 4 of 16

23284277, 2025, 10, Downloaded from https://agupubs.onlinelibrary.wiley.com/doi/10.1029/2025EF006367 by Chalmers University Of Technology, Wiley Online Library on [29/10/2025]. See the Terms and Conditions

(https://onlinelibrary.wiley.com/terms-and

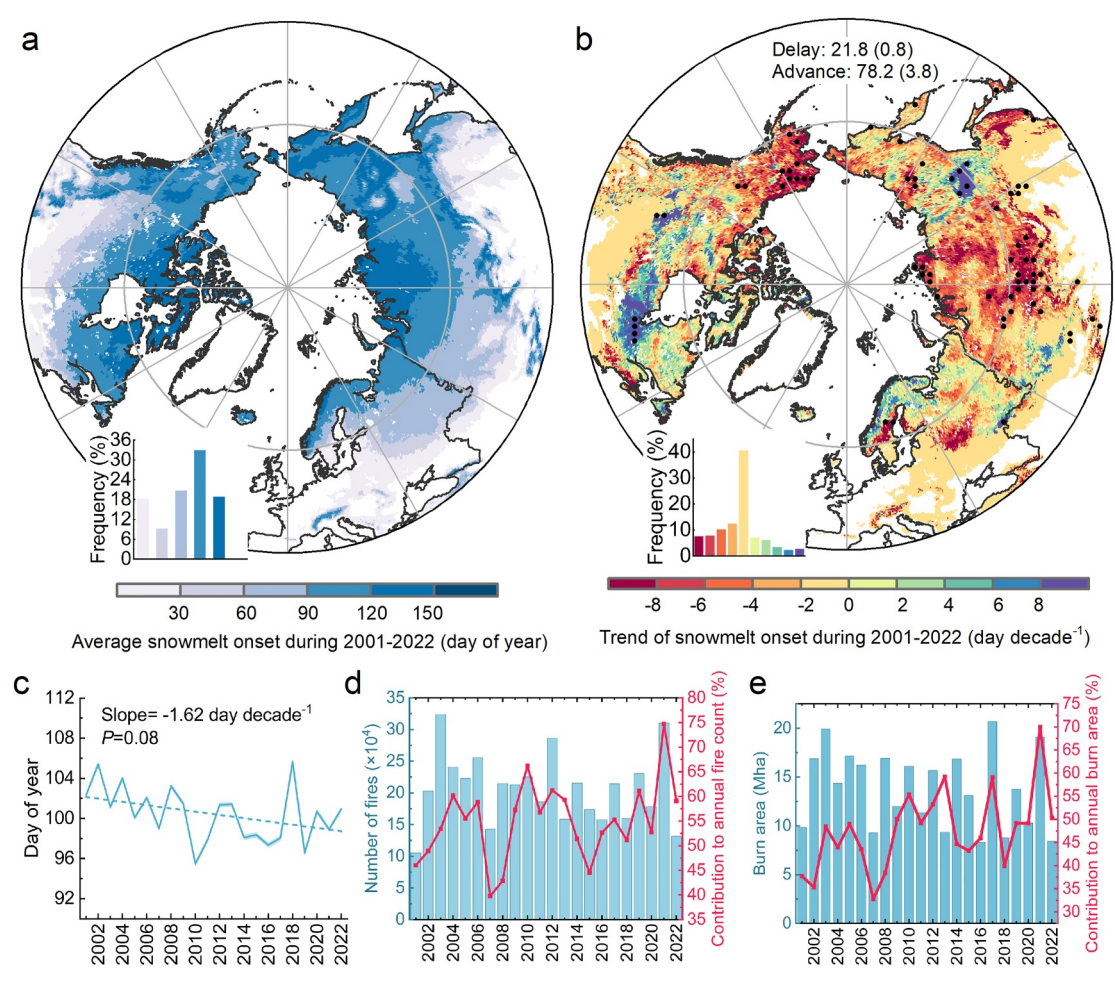


Figure 1. Spatiotemporal changes in the onset of snowmelt and the number of wildfire events and burned area during the post-snowmelt period during 2001-2022. (a) Spatial pattern of average snowmelt onset during 2001-2022 extracted from the ERA5-Land snow water equivalent (SWE) product. (b) Spatial pattern of change in snowmelt onset during 2001-2022. The top numbers denote the areal proportions of onset of the snowmelt with delayed and advanced trends, while the numbers in the parentheses denote the areal proportions of onset of snowmelt with significant trends (P < 0.05). The black dots indicate statistically significant trends (P < 0.05). The insets present the histograms for the values. (c) The overall average trend of the onset of snowmelt during 2001-2022. (d) Number of wildfire events on land covered with natural vegetation during the post-snowmelt period and its contribution to the annual number of fire events. (e) Burned area for land covered with natural vegetation during the post-snowmelt period and its contribution to the annual burned area. The day of the calendar year (rather than snow year) was adopted as the temporal reference for reporting snowmelt onset dates.

# 3. Results and Discussions

# 3.1. Spatiotemporal Patterns of Snowmelt Onset and Growing Concern About Post-Snowmelt Wildfires

The snowmelt onset date derived from ERA5-Land SWE data reveals that the onset of snowmelt mainly occurred before May, with approximately 72.3% of the regions with snowmelt occurring during the spring (Figure 1a). As expected, the snowmelt onset generally occurred later at higher latitudes. Over the last two decades, widespread shifts toward earlier melting dates were observed across 78.1% of the study area, and pixels with significant (P < 0.05) advancement of snowmelt onset were mainly concentrated in central Russia and northern Alaska (Figure 1b). On average, the snowmelt onset advanced at a rate of 1.6 days per decade, although this trend was not statistically significant (P = 0.08; Figure 1c). The shift in snowmelt onset trend was aligned with findings from previous studies conducted in whole Northern Hemisphere (Li & Fan, 2025; Mioduszewski et al., 2015; Riihel, 2019; J. Zheng et al., 2022; L. Zheng et al., 2022), Alaska (J. Zheng et al., 2022; L. Zheng et al., 2022), Arctic areas (Wang et al., 2013), western United States (O'Leary et al., 2020), and Mongolia (Li et al., 2025), while the specific magnitude of trends may vary due to the differences in study period to estimate the trend, data source, and the methodology employed for snowmelt onset extraction.

XU ET AL. 5 of 16

For land covered with natural vegetation, the average annual burned area during the post-snowmelt period was 13.2 Mha yr<sup>-1</sup> between 2001 and 2022, accounting for 47.6% of the annual burned area in this region (Figure 1e). Similarly, the cumulative number of wildfire events on land covered with natural vegetation after snowmelt accounted for 55.0% of the annual number of wildfire events (Figure 1d). In addition, the burned area and number of wildfire events during the post-snowmelt period made increasing contributions to the annual total estimates between 2001 and 2022 (Figures 1d and 1e), indicating the importance of clarifying the response of wildfires to earlier snowmelt.

We also observed advanced snowmelt onset spatially from our analyses of the GLDAS SWE product and the brightness temperature data set (Figures S3-S4 in Supporting Information S1). Regarding the snowmelt onset extracted from GLDAS SWE and the temperature brightness data set, separately, no significant advancing trends in the snowmelt onset were observed overall during 2004–2022 (Figure S3c in Supporting Information S1) and 2001–2022 (Figures S4c in Supporting Information S1), respectively. In addition, the GLDAS SWE-based estimates revealed that 58.2% of the regions exhibited the advanced trends, which is lower than that of ERA5 Land SWE-based estimates (Figures S3b in Supporting Information S1). These discrepancies between the GLDAS and ERA5 Land SWE-based snowmelt onset estimates may likely be attributed to differences in the study periods, the differences in masked regions where there was low SWE or no persistent snow cover, and the differences in the methodologies for generating SWE in two data sets (Shao et al., 2022). The differences between the brightness temperature and ERA5 Land SWE-based estimates may arise from the data availability constraints induced inconsistent regions analyzed, as well as the differences in the methodologies used for snowmelt onset extraction. In terms of snowmelt onset extraction methodology, the SWE-based method determines snowmelt onset by identifying peak snow water equivalent, which marks the transition from accumulation to ablation phases according to mass balance principles (Fontrodona-Bach et al., 2023). In comparison, the brightness temperature method relies on microwave signal variations, particularly the characteristic rapid decrease in TbD that physically corresponds to liquid water formation in surface snow layers (Wang et al., 2013, 2016).

# 3.2. Interannual Variability in Snowmelt Onset is Critically Associated With the Occurrence of Post-Snowmelt Wildfires

The partial correlation analysis suggests that negative correlations between snowmelt onset extracted from ERA5-Land SWE product and the number of wildfire events (burned area) during the post-snowmelt period were observed in more than 75.9% (74.5%) of the analyzed pixels, with over 41.1% (39.3%) of analyzed pixels exhibiting significant (P < 0.05) correlations (Figure 2). This indicates that an earlier snowmelt onset facilitated the occurrence of post-snowmelt wildfires. Positive correlations between snowmelt onset and the number of wildfire events (burned area) during the post-snowmelt period were observed in only about 24.1% (25.5%) of the analyzed pixels, with about 5.4% (6.6%) of the pixels exhibiting significant correlations. Similar partial correlations between snowmelt dates and wildfire dynamics were obtained for the use of  $7 \times 7$  and  $11 \times 11$  moving windows (Figure S5 in Supporting Information S1) and also for our analyses based on the GLDAS SWE and brightness temperature data sets (Figure S6 in Supporting Information S1).

# 3.3. Potential Intermediate Processes Connecting Snowmelt Onset With Occurrence of Post-Snowmelt Wildfires

Partial correlation analysis revealed significant negative correlations between snowmelt onset derived from ERA5-Land SWE product and these intermediate processes (i.e., VPD, CWD, and BUI), and significant positive correlations between these processes and the number of wildfire events and burned area during the post-snowmelt period within a 9 × 9-pixel moving window (Figure S7 in Supporting Information S1). Consistent partial correlations were obtained based on the GLDAS SWE product and brightness temperature data set (Figures S8–S9 in Supporting Information S1). The results were consistent with the hypothesis that earlier snowmelt onset tends to increase atmosphere dryness, plant water stress, and fuel moisture content and fuel availability, providing favorable conditions for wildfire occurrence and spread. To further quantify the contributions of the three intermediate processes associated with snowmelt onset to the number of wildfire events and burned area, we employed a structural equation model (SEM) to assess each pathway (Figure 3 and Figure S10 in Supporting Information S1). Overall, the EAR5-Land-based estimates within a 9 × 9-pixel moving window revealed that over 78.9% of the analyzed pixels are with AGFI > 0.9, TLI > 0.95, P > 0.05, and  $\chi 2/df < 3$  (Figure S11 in Supporting Information S1), demonstrating the suitability of our SEM for studying the pathways.

XU ET AL. 6 of 16

23284277, 2025, 10, Downloaded from https://agupubs.onlinelibrary.wiley.com/doi/10.1029/2025EF006367 by Chalmers University Of Technology, Wiley Online Library on [29/10/2025]. See the

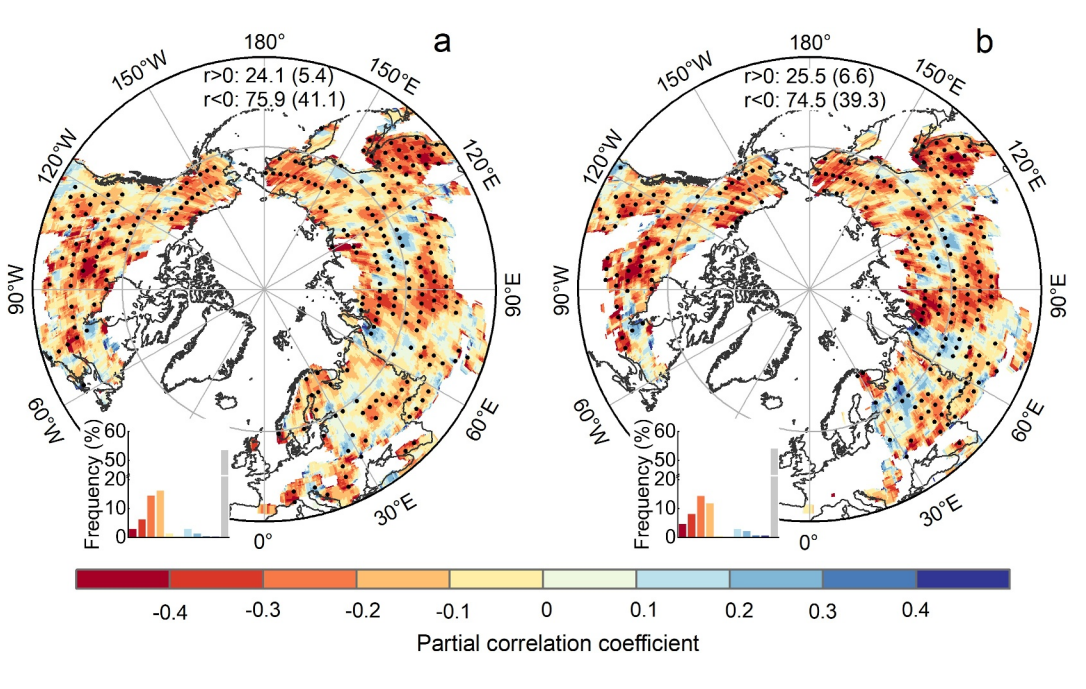


Figure 2. Partial correlation coefficients between the snowmelt onset date and cumulative (a) number of wildfire events and (b) burned area during the post-snowmelt period using a  $9 \times 9$ -pixel moving window. The snowmelt onset date was extracted from the ERA5-Land snow water equivalent (SWE) product. The black dots indicate significant partial correlations (P < 0.05). The numbers in the top denote the area proportions with positive (r > 0) and negative (r < 0) correlations, and the number in the parentheses denotes the area proportions with significant correlations. The insets present the histograms for the correlation coefficients, with the gray bar denoting the area proportions of statistically insignificant correlation coefficients.

The spatial patterns of the path effect derived from ERA5-Land based estimates indicate that the shifts in snowmelt onset mainly post negative impacts on the number of wildfire events during the post-snowmelt period through VPD, CWD, and BUI in 72.2%, 60.7%, and 61.1% of the northern latitudes, respectively (Figures 3b-3d, and Figure S12 in Supporting Information S1). This indicated that an earlier snowmelt may increase the postsnowmelt incidence. Notably, the pathway analysis revealed that the snowmelt onset, through VPD, is associated with the largest path effect size on the number of wildfire events. Specifically, the average path effect of snowmelt onset on the number of wildfire events through VPD was the strongest (-0.16), contributing 57.1% of the overall path effect. This effect more than doubled that observed through CWD (-0.06) and BUI (-0.06; Figure 3e). The path effect through VPD was also spatially the most extensive, encompassing 47.5% of the study area, whereas that through CWD and BUI contributed roughly equivalent proportions, covering 25.9% and 26.6% of the study area, respectively (Figure 3a). In terms of each land cover type, VPD consistently serves as the most robust statistical predictor of the path effect between snowmelt onset and the number of wildfire events during post-snowmelt period, contributing over 48.5% of the corresponding total path effect. The only exceptions occurred in deciduous needleleaf forests, where BUI shows the greatest effect size, contributing over 47.0% of the total path effect, and in shrublands, where CWD contributes most significantly to the path effect, contributing over 51.9% of the total path effect (Figure 4a).

In each dominant pathway, defined as the pathway with the strongest path effect, the path effect of shifts in snowmelt onset derived from the ERA5 Land SWE product on the post-snowmelt wildfires showed a clear dependence on aridity (Figures 5b–5d). Compared with arid regions, humid regions exhibited higher area proportions of the negative path effect, indicating that an earlier snowmelt onset tended to result in a greater increase in post-snowmelt wildfires in humid regions than in arid regions. Moving from arid to humid regions, the area proportion where the intermediate effect of VPD increased the number of wildfire events during the post-snowmelt period rose from 72.6% to 85.5% (Figure 5d). Similarly, for CWD, this proportion increased from 56.8% to 76.8%, and for BUI, it rose from 50.7% to 82.0% (Figure 5d). This occurred primarily because, in more humid regions, areas where shifts in snowmelt onset negatively influence the VPD, CWD, and BUI were more prevalent (Figure 5b). Moreover, in more humid regions, the VPD, CWD, and BUI had a more widespread positive effect on the number of wildfire events during the post-snowmelt period (Figure 5c). Among different

XU ET AL. 7 of 16

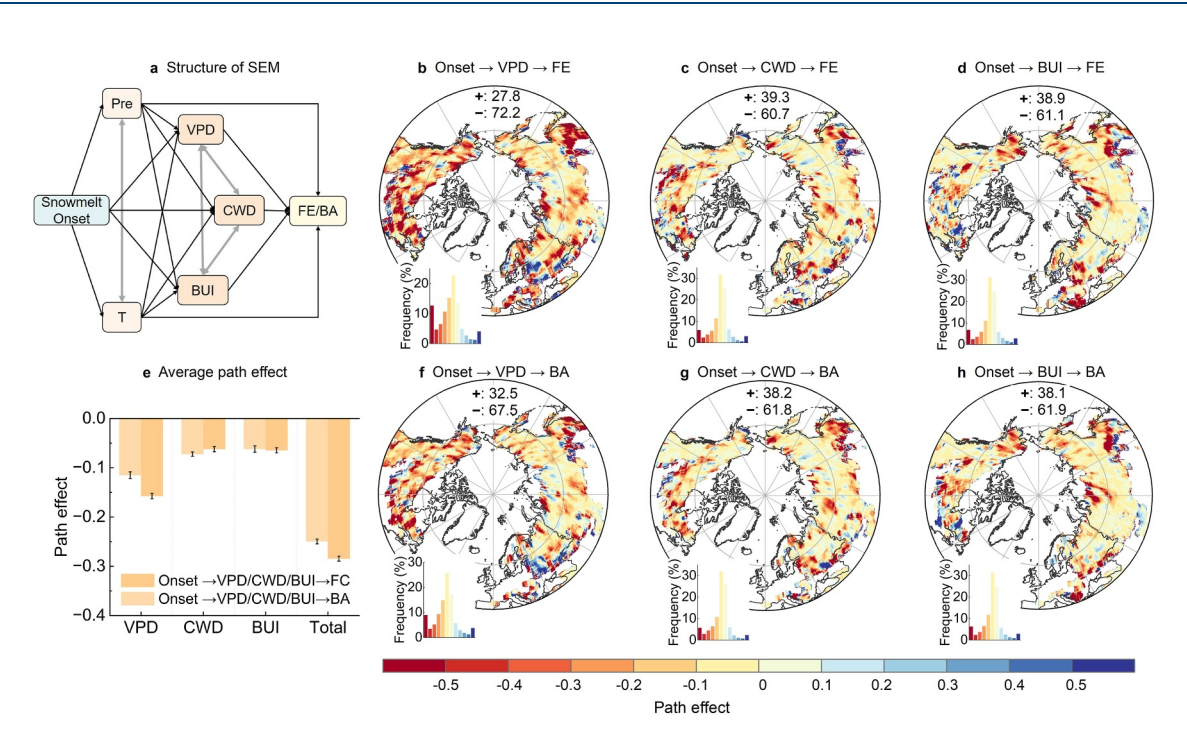


Figure 3. Pathway analysis of the potential mechanisms underlying the linkage between the onset of snowmelt and the number of wildfire events (FE) and burned area (BA) via vapor pressure deficit (VPD), climatic water deficit (CWD), and buildup index (BUI). (a) Conceptual structural equation model (SEM) depicting the path effect of the onset of snowmelt on FE and BA. (b–d, f–h), Spatial pattern of the path effect of the onset of snowmelt in terms of the FE (b–d) and BA (f–h) during the post-snowmelt period via linkages with VPD (b, f), CWD (c, g), and BUI (d, h). The numbers on the top denote the area proportions with positive (+) or negative (-) path effect. The inserts present the histograms for the path effect (e.g., Onset $\rightarrow$ VPD $\rightarrow$ FE), which was the indirect effect of the snowmelt onset on FE during the post-snowmelt period via VPD, and was estimated as the product of the direct effect of snowmelt onset on VPD and the direct effect of VPD on FE. e, Average path effect of the linkage between the onset of the snowmelt and the FE and BA during the post-snowmelt periods via VPD, CWD, and BUI, respectively. The error bar denotes the 95% confidence interval for the average path effect. The snowmelt onset dates were derived from the ERA5-Land SWE product. The pathway analysis was conducted using all burned pixels within a 9  $\times$  9-pixel moving window.

land cover types, except for deciduous needleleaf forests and shrubland, the area proportion of the negative path effect of snowmelt onset on post-snowmelt wildfire through VPD was largest (Figure 6c). This emerged because of the more prevalent negative influence of shifts in snowmelt onset on VPD (Figure 6a), and a more widespread

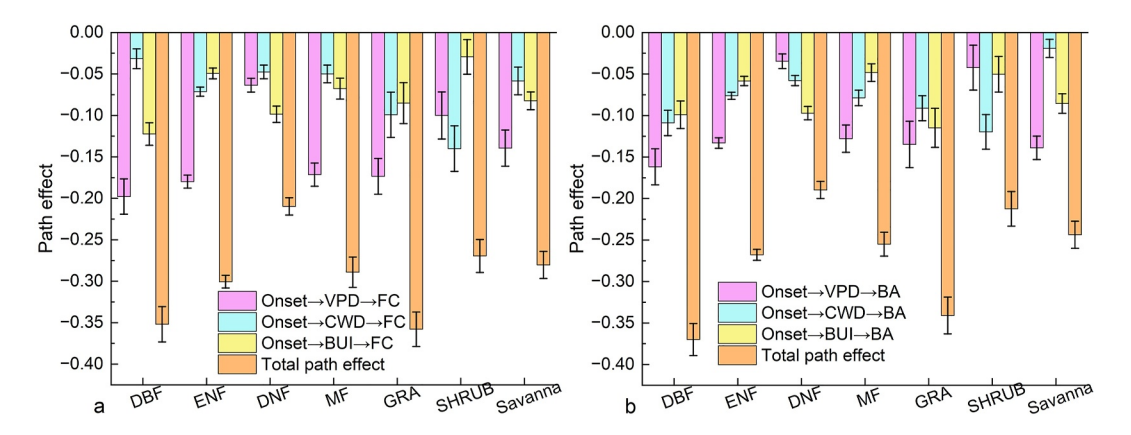


Figure 4. Statistical profiles of the average path effect of the linkage between the onset of the snowmelt and (a) the number of wildfire events (FE) and (b) burned area (BA) via vapor pressure deficit (VPD), climatic water deficit (CWD), and buildup index (BUI) in different land cover types, respectively. The error bar denotes the 95% confidence interval for the average path effect. The path effect (e.g., Onset $\rightarrow$ VPD $\rightarrow$ FE) was the indirect effect of the snowmelt onset on FE during the post-snowmelt period via VPDs, which was estimated as the product of the direct effect of snowmelt onset on VPD and the direct effect of VPD on FE. The snowmelt onset dates were derived from the ERA5-Land SWE product. The pathway analysis was conducted using all burned pixels within a 9  $\times$  9-pixel moving window. DBF, Deciduous broadleaf forest; ENF, Evergreen needleleaf forest; DNF, Deciduous needleleaf forest; MF, Mixed forest; GRA, Grassland; SHRUB, Shrubland.

XU ET AL. 8 of 16

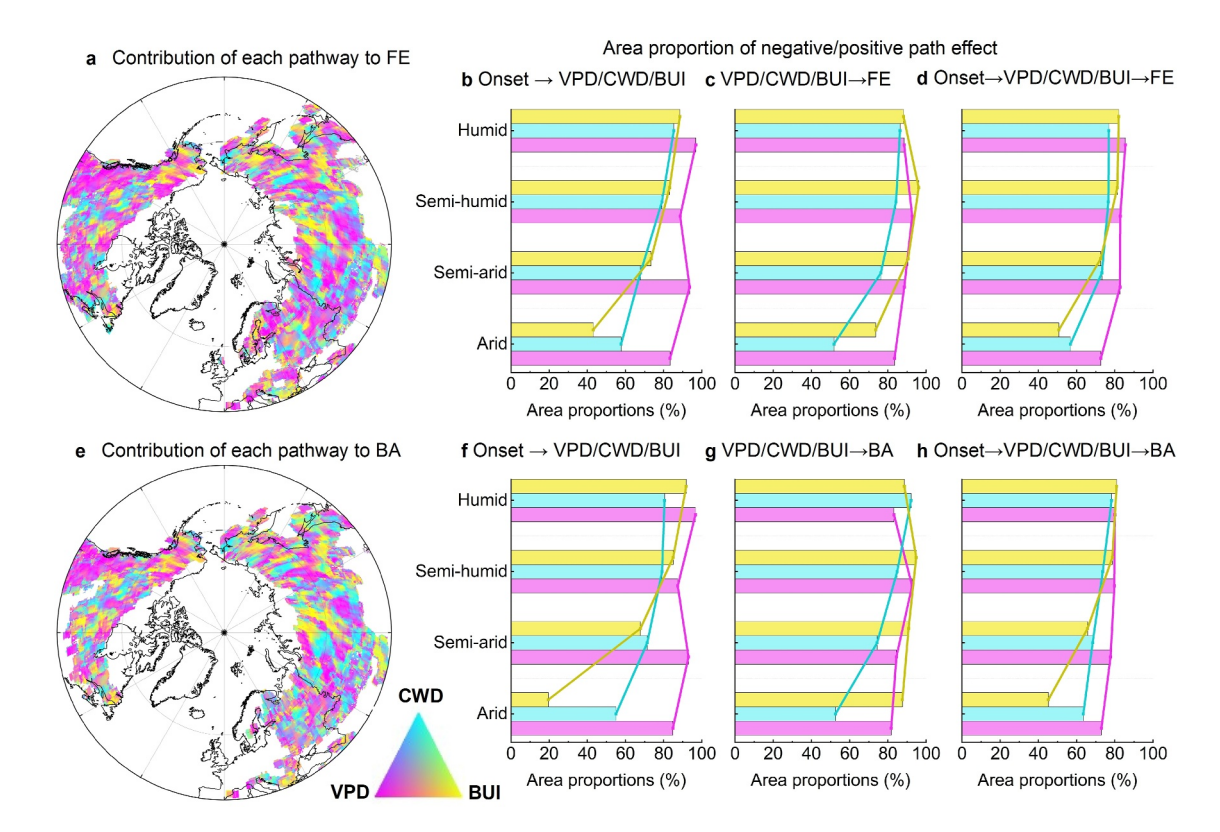


Figure 5. Spatial and statistical profiles of the path effect of the onset of the snowmelt to the number of fire events and burned area via vapor pressure deficit (VPD), climatic water deficit (CWD), and buildup index (BUI). (a, e) Spatial pattern of the contributions of VPD (magenta), CWD (cyan), and BUI (yellow) caused by shifts in snowmelt onset to the FE (a) and BA (e) during the post-snowmelt period. (b–d, f–h) Area proportion of negative path effect between the onset of snowmelt and FE (b–d) and BA (f–h) via the three intermediate processes in arid (aridity index (AI) < 0.2), semi-arid ( $0.2 \le AI < 0.5$ ), semi-humid ( $0.5 \le AI < 0.65$ ), and humid (AI  $\ge 0.65$ ) regions, including the area proportion of negative path effect between the onset of the snowmelt and intermediate processes (VPD, CWD, and BUI) (b) for FE and (f) for BA), between the onset of the snowmelt and the FE (d) and BA (h) via the three intermediate processes during the post-snowmelt period, and the area proportion of positive path effect between the three intermediate processes and FE (c) and BA (g) during the post-snowmelt period. The snowmelt onset dates were derived from the ERA5-Land SWE product. The structural equation model (SEM) was constructed using all burned pixels within a  $9 \times 9$ -pixel moving window.

positive effect of VPD on wildfires during the post-snowmelt period (Figure 6b). However, in deciduous needleleaf forests (shrubland), the largest area proportion of negative association occurred through BUI (CWD), because BUI (CWD) was more obviously negatively influenced by shifts in snowmelt onset (Figure 6a) and more positive effect on post-snowmelt wildfires (Figure 6b). We achieved consistent results from the pathway analyses between snowmelt onset and burned area from our analyses of the GLDAS SWE product and temperature brightness data set, and also for the use of different sizes of moving windows (Figures S12–S30 in Supporting Information S1).

#### 3.4. Potential Mechanisms for the Escalating Effect of Shifts in Snowmelt Onset on Wildfire Dynamics

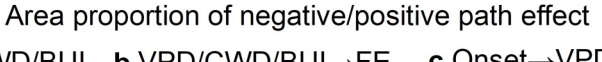
To explore the deep mechanisms associated with the critical impact of the shift in snowmelt onset on postsnowmelt wildfires via VPD and the other two intermediate pathway processes, we examined the changes in possible processes or variables related to each intermediate pathway process (Figure 7 and Figure S31 in Supporting Information S1), and compared the related shifts of the variables in regions with earlier and later snowmelt onset dates derived from ERA5 Land product (Figure 8 and Figure S32 in Supporting Information S1).

Generally, an earlier snowmelt onset triggers earlier seasonal phenological events (Billings & Bliss, 1959; Inouye & McGuire, 1991; Slatyer et al., 2021) and regulates water circulation through vegetation during the subsequent season (Guan et al., 2022; Slatyer et al., 2021; Vavrus, 2007), thereby increasing the vegetation water deficit and atmospheric dryness during the peak growing season. Specifically, higher temperatures not only cause snow to melt earlier but also advance the growing season (Figure S31d in Supporting Information S1), leading to earlier soil moisture consumption (Figures 8a and 8b). This, in combination with a large moisture demand from increased

XU ET AL. 9 of 16

23284277, 2025, 10, Downloaded from https://agupubs

om/doi/10.1029/2025EF006367 by Chalmers University Of Technology, Wiley Online Library on [29/10/2025]. See the Terms:



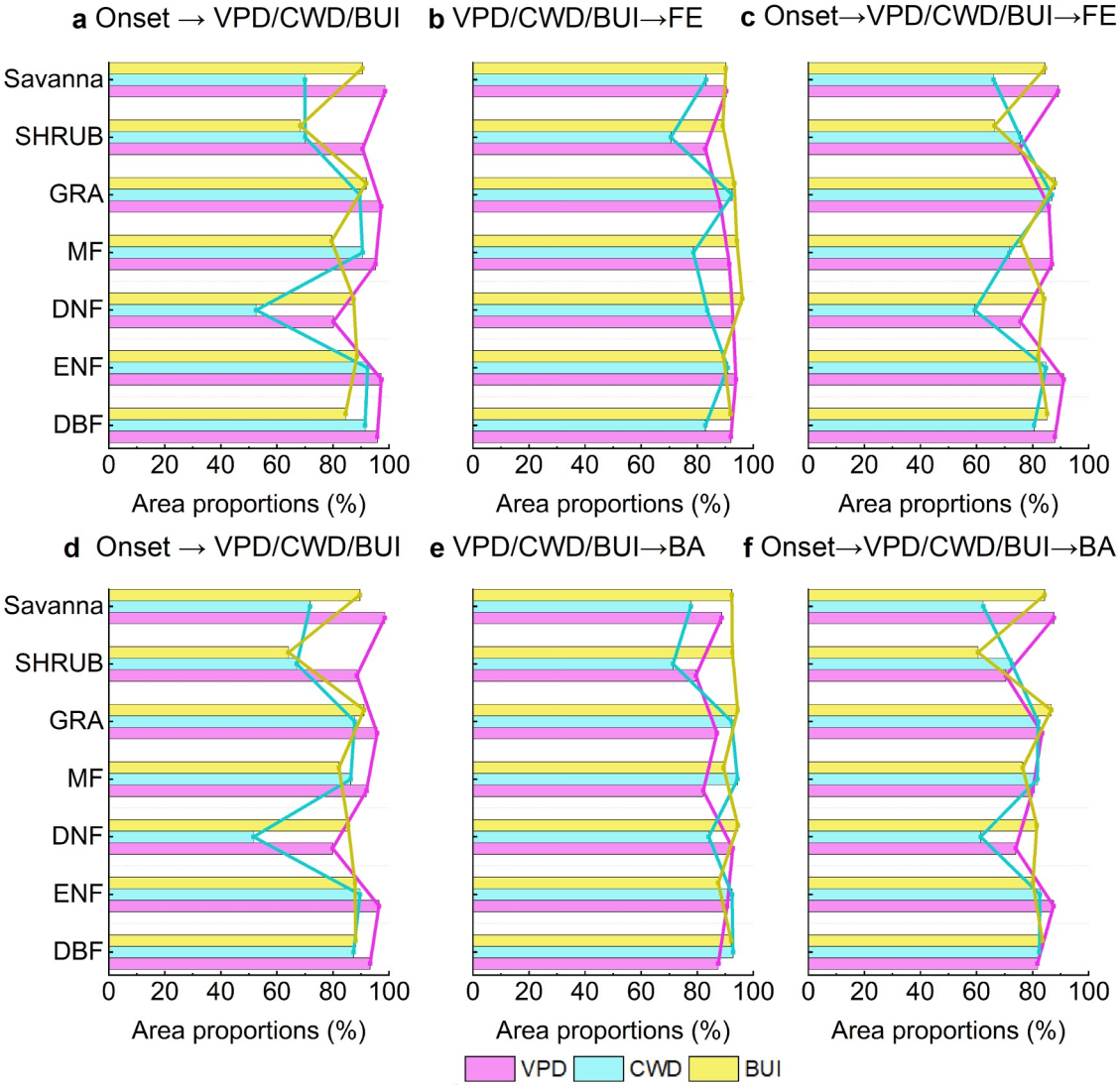


**Figure 6.** Statistical profiles of the path effect of the onset of the snowmelt on the number of fire events and burned area via vapor pressure deficit (VPD), climatic water deficit (CWD), and buildup index (BUI) in different land cover types. (a–c, d–f) Area proportion of negative path effect between the onset of snowmelt and FE (a–c) and BA (d–f) via the three intermediate processes in different land cover types, including the area proportion of negative path effect between the onset of the snowmelt and intermediate processes (VPD, CWD, and BUI) (a for FE and d for BA), between the onset of the snowmelt and the FE (b) and BA (e) via the three intermediate processes during the post-snowmelt period, and the area proportion of positive path effect between the three intermediate processes and FE (c) and BA (f) during the post-snowmelt period. The snowmelt onset dates were derived from the ERA5-Land SWE product. The structural equation model (SEM) was constructed using all burned pixels within a 9 × 9-pixel moving window. DBF, Deciduous broadleaf forest; ENF, Evergreen needleleaf forest; DNF, Deciduous needleleaf forest; MF, Mixed forest; GRA, Grassland; SHRUB, Shrubland.

vegetation productivity (Figures 7a and 8a), results in a greater decrease in soil moisture during the summer and a larger climatic water deficit compared to areas with later snowmelt onset dates (Figures 8b and 8c). The post-snowmelt period consequently exhibits reduced soil moisture availability and heightened plant water stress, which suppresses evaporative cooling while boosting sensible heat flux (Figures 8d and 8e). This thermal feedback elevates local air temperatures (Seneviratne et al., 2010; Zona et al., 2022) and consequently increases VPD (Figures S8f, S33b and S33c in Supporting Information S1).

In addition to the water cycle, the impacts of shifts in snowmelt onset on post-snowmelt wildfires may also involve energy cycles. Specifically, earlier snowmelt induces a premature reduction in surface albedo (Figure S32b in Supporting Information S1), significantly enhancing absorption of downward shortwave radiation during

XU ET AL. 10 of 16

23284277, 2025, 10, Downloaded from https://suppubs.onlinelibrary.wiley.com/doi/10.1029/2025EP006367 by Chalmers University Of Technology, Wiley Online Library on [29/10/2025]. See the Terms and Conditions (https://onlinelibrary.wiley.com/terms-and-conditions) on Wiley Online Library for rules of use; OA articles are governed by the applicable Centwieron and Conditions (https://onlinelibrary.wiley.com/terms-and-conditions) on Wiley Online Library for rules of use; OA articles are governed by the applicable Centwieron and Conditions (https://onlinelibrary.wiley.com/terms-and-conditions) on Wiley Online Library for rules of use; OA articles are governed by the applicable Centwieron and Conditions (https://onlinelibrary.wiley.com/terms-and-conditions) on Wiley Online Library for rules of use; OA articles are governed by the applicable Centwieron and Conditions (https://onlinelibrary.wiley.com/terms-and-conditions) on Wiley Online Library for rules of use; OA articles are governed by the applicable Centwieron and Conditions (https://onlinelibrary.wiley.com/terms-and-conditions) on Wiley Online Library for rules of use; OA articles are governed by the applicable Centwieron and Conditions (https://onlinelibrary.wiley.com/terms-and-conditions) on Wiley Online Library for rules of use; OA articles are governed by the applicable Centwieron and Conditions (https://onlinelibrary.wiley.com/terms-and-conditions) on the applicable Centwieron

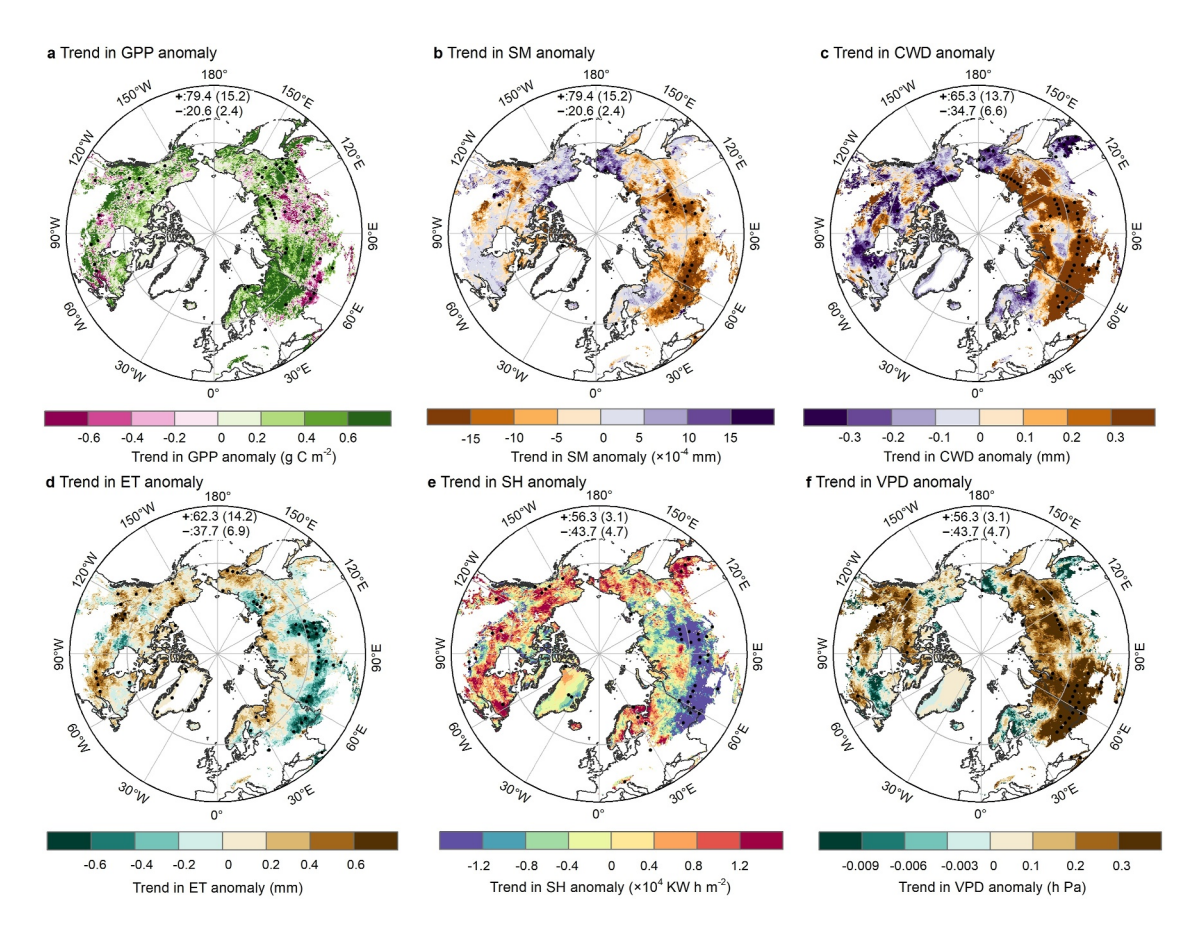
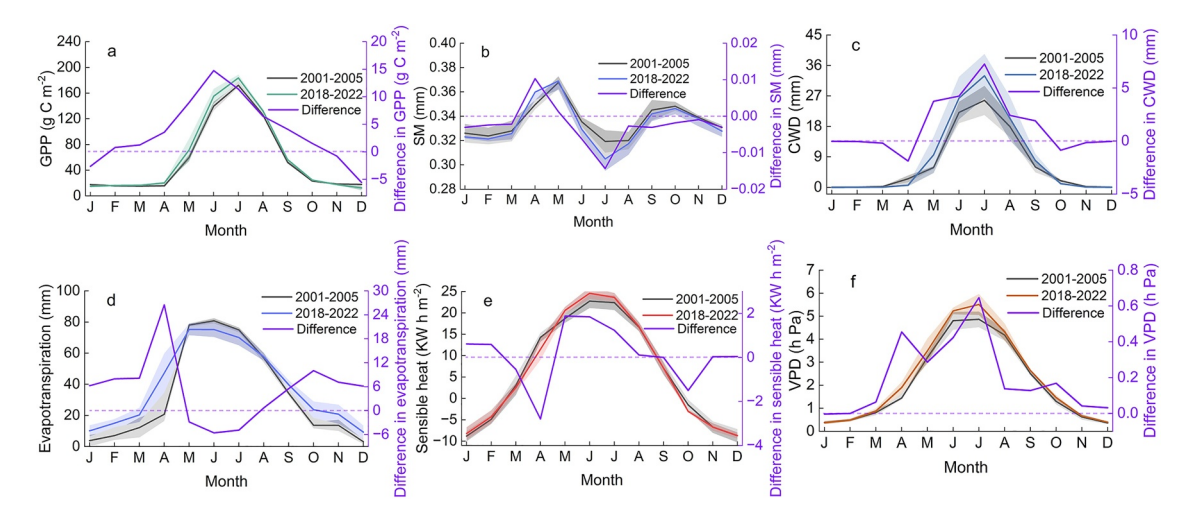


Figure 7. Spatial patterns of the trends of the anomalies in the environment variables. (a) gross primary production (GPP); (b) soil moisture; (e) climatic water deficit (CWD); (d) evapotranspiration (ET); (e) sensible heat flux (SH); (f) vapor pressure deficit (VPD). The black dots indicate the regions with significant trends (P < 0.05). The numbers in the top denoted the proportions of the areas in which increasing (+) or decreasing (-) trends, and the number in the bracket denoted the areal proportions of significant trends.



**Figure 8.** Comparisons of the monthly average values of the environment variables for early and late snowmelt onset dates. (a) gross primary production (GPP); (b) soil moisture (SM); (c) climatic water deficit (CWD); (d) evapotranspiration; (e) sensible heat flux, (f) vapor pressure deficit (VPD). To reduce noises and make robustness estimates, we calculated the values of the above variables between five pairs of years (2001 and 2018, 2002 and 2019, 2003 and 2020, 2004 and 2021, and 2005 and 2022). For each pair, we used pixels with significantly advanced snowmelt onset dates, and other pixels that experienced earlier snowmelt onset dates than the former pixels. Finally, we averaged the five pairs to report our estimates. The shaded area denotes the 95% confidence interval.

XU ET AL. 11 of 16

23284277, 2025, 10, Downloaded from https://agupubs.onlinelibrary.wiley.com/doi/10.1029/2025EF006367 by Chalmers University Of Technology, Wiley Online Library on [29/10/2025].

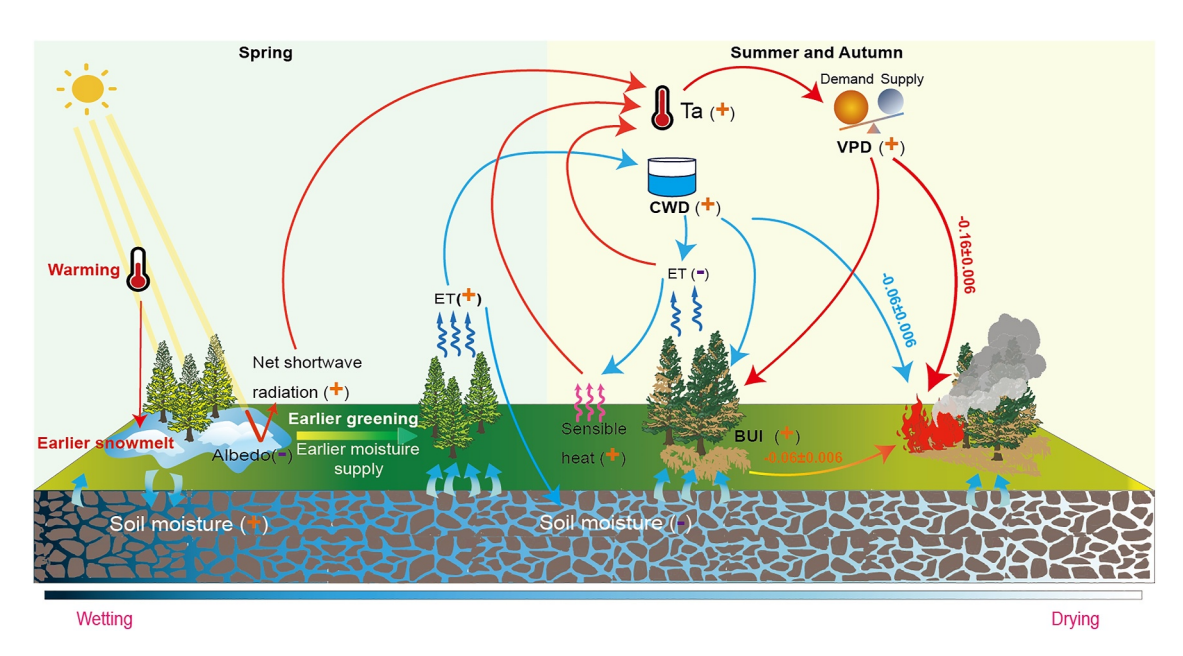


**Figure 9.** Schematic diagram of the facilitating role of earlier snowmelt onset on post-snowmelt wildfires via vapor pressure deficit (VPD), climatic water deficit (CWD), and buildup index (BUI). ET denotes evapotranspiration and Ta denotes air temperature. The number on each arrow represents the average path effect of the shifts in snowmelt onset on the number of wildfire events derive from structural equation model constructed within a 9 × 9-pixel moving window.

post-snowmelt period (Figures S31c and S32d in Supporting Information S1). The resultant energy surplus creates a positive feedback loop that further elevates temperatures (Figure S33a in Supporting Information S1) and VPD. As a result, an earlier may alter water and energy processes, contributing to increased VPD, ultimately establishing favorable conditions for wildfire ignition and spread.

To respond to increased atmosphere dryness and plant water stress (Figures 8c and 8f) and to enable plants to complete their life cycle within the current and the following growing seasons, plants induce leaf senescence and abscission by redistributing nutrients to reproductive organs and eliminating water consumption in older, less-productive leaves (Gan & Amasino, 1997; Munné-Bosch & Alegre, 2004; Ono et al., 2001). This ultimately contributes to the decreased fuel moisture content and increased fuel availability for wildfires (Figure 9 and Figures S31e and S32e in Supporting Information S1).

It should also be noted that, in addition to creating favorable burning conditions, an earlier snowmelt onset extends the period of surface exposure, thereby widening the temporal window for wildfire occurrence and contributing to increased wildfire activity.

While this study focuses on climatic drivers, shifts in ignition patterns—both natural and human-caused—induced by earlier snowmelt may also contribute to the observed increase in wildfires during the post-snowmelt period. For natural ignitions, rising global warming has been linked to higher thunderstorm frequency and lightning strikes (Chen et al., 2021; Goulden et al., 2017; Qie et al., 2022), elevating the likelihood of dry fuel ignition. In addition, human-ignited wildfires account for a substantial proportion of total wildfires, particularly in regions like North America (Abatzoglou, Balch, et al., 2018; Abatzoglou, Dobrowski, et al., 2018; Balch et al., 2017; Emily et al., 2018). Earlier snowmelt facilitates earlier human access to land for outdoor recreation and agricultural activities (O'Toole et al., 2019; Prbstl-Haider et al., 2021; Kutlu et al., 2025), thereby increasing probabilities for accidental or intentional wildfire starts. However, due to limited data on the long-term spatial and temporal observations of natural and human ignitions, the influence of earlier snowmelt on post-snowmelt wildfire dynamics through altered ignition regimes remains poorly quantified in this study. Future research should focus on generating long-term explicit data on ignition patterns using multiple data sources and advanced methodology, and quantifying the role of ignition pattern shifts driven by earlier snowmelt in shaping wildfire dynamics.

It should be noted that, while the year-to-year variation metric employed in this study effectively isolates interannual signals and captures short-term variability, it may not fully account for the cumulative effects of

XU ET AL. 12 of 16

23284277, 2025, 10, Downlo.

sustained multi-year snowmelt trends on post-snowmelt burning conditions (e.g., fire weather, vegetation dryness, and fuel availability). In addition, the average/cumulative values of burning conditions over the post-snowmelt period were considered in this study, which may mask the influence of intra-seasonal extremes in burning conditions. For instance, heavy rainfall events during this period could temporarily moisten fuels and reduce wildfire risk, thereby weakening the linkage between the snowmelt onset and subsequent wildfire activity. Future research should focus on assessing these long-term, snowmelt-driven influences on wildfire dynamics through their regulation of burning conditions, and carefully considering extreme climate events.

### 3.5. Implications of the Effect of Earlier Snowmelt Onset on Post-Snowmelt Wildfires

We highlighted the widespread advance of snowmelt has potentially escalated wildfire dynamics in the northern mid-to-high latitudes (>40°N), primarily through the elevated VPD induced by earlier snowmelt. The mechanisms revealed in this study have significant implications for assessing wildfire risks and modeling wildfires in regions vulnerable to ongoing and future climate change.

Firstly, our study offers a deeper insight into wildfire risks under climate change. With the progressing climate change, temperatures are expected to rise more rapidly in northern latitudes ( $>40^{\circ}N$ ) than elsewhere due to the amplifying effects of positive feedbacks (Rantanen et al., 2022). This warming will result in an even earlier snowmelt onset and broader areas without snow cover (Klein et al., 2016; Xiao, 2021). As underscored in this study, an earlier snowmelt onset leads to a widespread increase in wildfire disturbances during the post-snowmelt period. Additionally, the loss of the snowpack exposes the land surface and heightens the risk of wildfire disturbance (Kampfa et al., 2022). Therefore, our findings are valuable for estimating wildfire risks under climate change.

Secondly, our results are beneficial for enhancing regional wildfire simulations. Dynamic global vegetation models (DGVMs) can simulate wildfires by incorporating key processes and variables related to wildfire dynamics within the context of global vegetation and climatic interactions. Factors such as fuel availability, ignition sources, weather conditions, and landscape features are considered to simulate the ignition, spread, and extinction of wildfires (Hantson et al., 2016). However, the influence of snowmelt onset on wildfires has not been previously considered due to a limited understanding of its specific effects. In this study, we demonstrated that an earlier snowmelt onset facilitates wildfire occurrences by promoting favorable fire weather and combustion conditions. This understanding paves the way for introducing new and refined dynamics and parameterizations into models, thereby enhancing the accuracy of wildfire simulations, and improving projections of carbon-climate feedbacks.

# 4. Conclusions

In this study, we found that interannual variability in snowmelt onset has far-reaching implications for influencing post-snowmelt wildfires. This influencing role was predominantly through the variations in snowmelt onset-induced VPD, which was the strongest statistical predictor influencing wildfire dynamics in about 47% of the northern latitudes (>40°N). The influencing role through VPD contributed about 57% of the total influencing role, which doubled that contributed by CWD or BUI. Our mechanistic analysis revealed that this was primarily due to the advances of snowmelt-induced earlier spring vegetation green-up and premature moisture consumption, which heightened plant water deficits. This heightened deficit also resulted in limited evaporative cooling and increased sensible heat fluxes, which further raised the local air temperature, thereby increasing VPD and providing favorable conditions for wildfire. Our results provide new insights into the impact of climate change on fire dynamics and can support data-driven and process-based models to consider the effects of earlier snowmelt, thereby improving fire simulations. Lastly, with the progression of global warming, snow is expected to melt earlier than ever before, which will further lead to favorable fire weather and burning conditions, thereby increasing the risk of wildfire occurrence.

#### **Conflict of Interest**

The authors declare no conflicts of interest relevant to this study.

XU ET AL. 13 of 16

23284277, 2025, 10, Downloaded from https://agupub

doi/10.1029/2025EF006367 by Chalmers University Of Technology, Wiley Online Library on [29/10/2025].

# **Data Availability Statement**

All of the data used in this study are freely and publicly accessible. The MCD64A1, ERA5-Land dataset are from Giglio et al. (2015) and Muñoz-Sabater et al. (2021), respectively, and is available at https://doi.org/10.5067/MODIS/MCD64A1.006 and Muñoz-Sabater (2019). The MCD12Q2 dataset is from Friedl et al. (2019) and available at https://lpdaac.usgs.gov/products/mcd12q2v006/, the TerraClimate dataset is from Abatzoglou, Balch, et al. (2018), Abatzoglou, Dobrowski, et al. (2018), and available at https://www.climatologylab.org/terraclimate.html, the GLDAS 2.2 dataset is from Li et al. (2019), and available at https://doi.org/10.5067/TXBMLX370XX8, the MCD14DL product is from Giglio et al. (2016) and available at https://firms.modaps.eosdis.nasa.gov/download/, the brightness temperature from SMMR, SSM/I, and SSMIS observations are from Maslanik and Stroeve (2004) and available at Bliss et al. (2022), the ESA CCI land cover maps are from ESA (2017) and available at https://www.esa-landcover-cci.org/?q=node/164, the grid GPP products are derived from Li and Xiao (2019) and available at https://globalecology.unh.edu/data/GOSIF-GPP.html, the buildup index product is from Kropp et al. (2022) and available at https://doi.org/10.24381/cds.0e89c522, and the aridity index data is from Zomer et al. (2022) and available at Trabucco and Zomer (2019).

#### Acknowledgments

This work was funded by the National Natural Science Foundation of China (Grant 42361144877). H.W.C and D.C. were supported by the Swedish strategic research area MERGE (ModElling the Regional and Global Earth system). This work was also supported by the State Key Laboratory of Earth Surface Processes and Resource Ecology (Grant 2023-KF-02) and the Third Xinjiang Scientific Expedition Program (Grant 2022xjkk0106). J.X. was supported by University of New Hampshire via bridge supports

#### References

- Abatzoglou, J. T., Balch, J. K., Bradley, B. A., & Kolden, C. A. (2018). Human-related ignitions concurrent with high winds promote large wildfires across the USA. *International Journal of Wildland Fire*, 27(6), 377–386. https://doi.org/10.1071/WF17149
- Abatzoglou, J. T., Dobrowski, S. Z., Parks, S. A., & Hegewisch, K. C. (2018). Terraclimate, a high-resolution global dataset of monthly climate and climatic water balance from 1958–2015. Scientific Data, 5(1), 170191. Article number: 17019. https://doi.org/10.1038/sdata.2017.191
- Balch, J. K., Bradley, B. A., Abatzoglou, J. T., Nagy, R. C., & Mahood, A. L. (2017). Human-started wildfires expand the fire niche across the United States. *Proceedings of the National Academy of Sciences of the United States of America*, 114(11), 2946–2951. https://doi.org/10.1073/pngs.1617394114
- Ban, Z., Xin, C., Fang, Y., Ma, X., Li, D., & Lettenmaier, D. P. (2023). Snowmelt-radiation feedback impact on Western U.S. Streamflow. Geophysical Research Letters, 50(23), e2023GL105118. https://doi.org/10.1029/2023GL105118
- Billings, W. D., & Bliss, L. C. (1959). An alpine snowbank environment and its effects on vegetation, plant development, and productivity. *Ecology*, 4(3), 388–397. https://doi.org/10.2307/1929755
- Bliss, A. C., Anderson, M., & Drobot, S. (2022). Snow melt onset over arctic sea ice from SMMR and SSM/I-SSMIS brightness temperatures. (NSIDC-0105, version 5) [Dataset]. NASA National Snow and Ice Data Center Distributed Active Archive Center. https://doi.org/10.5067/TRGWOONTOG5
- Chen, Y., Romps, D. M., Seeley, J. T., Veraverbeke, S., Riley, W. J., Mekonnen, Z. A., & Randerson, J. T. (2021). Future increases in Arctic lightning and fire risk for permafrost carbon. *Nature Climate Change*, 11(5), 404–410. https://doi.org/10.1038/s41558-021-01011-y
- Emily, F., Bethany, B., Abatzoglou, J. T., & Balch, J. (2018). Human-related ignitions increase the number of large wildfires across U.S. ecoregions. *Fire*, *I*(1), 4. https://doi.org/10.3390/fire1010004
- ESA. (2017). Land cover cci product user guide version 2.0 [Dataset]. Retrieved from http://maps.elie.ucl.ac.be/CCI/viewer/download/,ESACCI-LC-Ph2-PUGv2 2.0.pdf
- Flannigan, M. D., Logan, K. A., Amiro, B. D., Skinner, W. R., & Stocks, B. J. (2005). Future area burned in Canada. Climatic Change, 72, 1–16. https://doi.org/10.1007/s10584-005-5935-y
- Flannigan, M. D., Wotton, B. M., Marshall, G. A., de Groot, W. J., Johnston, J., Jurko, N., & Cantin, A. S. (2016). Fuel moisture sensitivity to temperature and precipitation: Climate change implications. *Climatic Change*, 134, 59–71. https://doi.org/10.1007/s10584-015-1521-0
- Fontrodona-Bach, A., Schaefli, B., Woods, R., Teuling, A. J., & Larsen, J. R. (2023). NH-SWE: Northern hemisphere snow water equivalent dataset based on in situ snow depth time series. *Earth System Science Data*, 15(6), 2577–2599. https://doi.org/10.5194/essd-15-2577-2023
- Forzieri, G., Miralles, D. G., Ciais, P., Alkama, R., Ryu, Y., Duveiller, G., et al. (2020). Increased control of vegetation on global terrestrial energy fluxes. *Nature Climate Change*, 10(4), 356–362. https://doi.org/10.1038/s41558-020-0717-0
- Friedl, M., Gray, J., & Sulla-Menashe, D. (2019). Mcd12q2 MODIS/Terra+Aqua land cover dynamics yearly L3 global 500m sin grid v006 [Dataset]. NASA Land Processes Distributed Active Archive Center. https://doi.org/10.5067/MODIS/MCD12Q2.006
- Gan, S., & Amasino, R. M. (1997). Making sense of senescence (molecular genetic regulation and manipulation of leaf senescence). Plant Physiology, 113(2), 313–319. https://doi.org/10.1104/pp.113.2.313
- Giglio, L., Justice, C., Boschetti, L., & Roy, D. (2015). Mcd64a1 MODIS/Terra+Aqua burned area monthly L3 global 500m sin grid v006 [Dataset]. NASA Land Processes Distributed Active Archive Center. https://doi.org/10.5067/MODIS/MCD64A1.006
- Giglio, L., Randerson, J. T., Van der Werf, G. R., Kasibhatla, P. S., Collatz, G. J., Morton, D. C., & DeFries, R. S. (2010). Assessing variability and long-term trends in burned area by merging multiple satellite fire products. *Biogeosciences*, 7(3), 1171–1186. https://doi.org/10.5194/bg-7-1171.2010
- Giglio, L., Schroeder, W., & Justice, C. O. (2016). The collection 6 MODIS active fire detection algorithm and fire products. Remote Sensing of Environment, 178(1), 31–41. https://doi.org/10.1016/j.rse.2016.02.054
- Goulden, M. L., Veraverbeke, S., Rogers, B. M., Jandt, R. R., Miller, C. E., Wiggins, E. B., & Randerson, J. T. (2017). Lightning as a major driver of recent large fire years in North American boreal forests. *Nature Climate Change*, 7, 529–534. https://doi.org/10.1038/nclimate3329
- Guan, X., Guo, S., Huang, J., Shen, J., Fu, L., & Zhang, G. (2022). Effect of seasonal snow on the start of growing season of typical vegetation in northern hemisphere. *Geography and Sustainability*, 3(3), 268–276. https://doi.org/10.1016/j.geosus.2022.09.001
- Hantson, S., Arneth, A., Harrison, S. P., Kelley, D. I., Prentice, I. C., Rabin, S. S., et al. (2016). The status and challenge of global fire modelling. Biogeosciences, 13(1), 3359–3375. https://doi.org/10.5194/bg-13-3359-2016
- Hu, L. T., & Bentler, P. M. (2009). Cutoff criteria for fit indexes in covariance structure analysis: Conventional criteria versus new alternatives. Structural Equation Modeling, 6(1), 1–55. https://doi.org/10.1080/10705519909540118
- Inouye, D. W., & McGuire, A. D. (1991). Effects of snowpack on timing and abundance of flowering in delphinium Nelsonii (Ranunculaceae): Implications for climate change. *American Journal of Botany*, 44(12), 6163–6172. https://doi.org/10.1002/j.1537-2197.1991.tb14504.x

XU ET AL. 14 of 16

23284277, 2025, 10, Downlo

- Jakobs, C. L. R., van den Broeke, C. H., van de Berg, M. R., & van Wessem, W. J. (2021). Spatial variability of the snowmelt-albedo feedback in Antarctica. *Journal of Geophysical Research*, 126(2), e2020JF005696. https://doi.org/10.1029/2020JF005696
- Jones, M. W., Abatzoglou, J. T., Veraverbeke, S., Andela, N., Lasslop, G., Matthias, F., et al. (2022). Global and regional trends and drivers of fire under climate change. Reviews of Geophysics, 60(3), e2020RG000726. https://doi.org/10.1029/2020RG000726
- Kampfa, S. K., McGrathb, D., Searsa, M. G., Fassnachta, S. R., Kiewieta, L., & Hammond, J. C. (2022). Increasing wildfire impacts on snowpack in the western U.S. Proceedings of the National Academy of Sciences of the United States of America, 119(39), e2200333119. https://doi.org/ 10.1073/pnas.2200333119
- Klein, G., Vitasse, Y., Rixen, C., Marty, C., & Rebetez, M. (2016). Shorter snow cover duration since 1970 in the Swiss Alps due to earlier snowmelt more than to later snow onset. Climatic Change, 139, 1–13. https://doi.org/10.1007/s10584-016-1806-y
- Koshkin, A. L., Hatchett, B. J., & Nolin, A. W. (2022). Wildfire impacts on Western United States Snowpacks. Frontiers in Water, 4, 971271. https://doi.org/10.3389/frwa.2022.971271
- Kropp, H., Loranty, M. M., Rutter, N., Fletcher, C. G., Derksen, C., Mudryk, L., & Todt, M. (2022). Are vegetation influences on arctic-boreal snow melt rates detectable across the northern hemisphere? *Environmental Research Letters*, 17(10), 104010. https://doi.org/10.1088/1748-9326/ac8fa7
- Kutlu, D., Kasalak, M. A., & Bahar, M. (2025). Assessing climate change impacts on outdoor recreation: Insights from visitor and business perspectives. Sustainability, 17(8), 3400. https://doi.org/10.3390/su17083400
- Lai, G., Li, J., Wang, J., Wu, C., Zhang, Y., Zohner, C. M., et al. (2024). Earlier peak photosynthesis timing potentially escalates global wildfires. National Science Review, 11(9), nwae292. https://doi.org/10.1093/nsr/nwae292
- Li, B., Rodell, M., Kumar, S., Beaudoing, H. K., Getirana, A., Zaitchik, B. F., et al. (2019). Global grace data assimilation for groundwater and drought monitoring: Advances and challenges. Water Resources Research, 55(9), 7564–7586. https://doi.org/10.1029/2018WR024618
- Li, D., Ouyang, W., Wang, L., Chen, J., Zhang, H., Sharkhuu, A., et al. (2025). Revisiting snowmelt dynamics and its impact on soil moisture and vegetation in mid-high latitude watershed over four decades. *Agricultural and Forest Meteorology*, 362, 110353. https://doi.org/10.1016/j.agrformet.2024.110353
- Li, D., Wrzesien, M. L., Durand, M., Adam, J., & Lettenmaier, D. P. (2017). How much runoff originates as snow in the Western United States, and how will that change in the future? *Geophysical Research Letters*, 44(12), 6163–6172. https://doi.org/10.1002/2017GL073551
- Li, X., & Fan, H. (2025). Characteristics of the spatiotemporal differences in snowmelt phenology in the northern hemisphere. *Journal of Hydrology: Regional Studies*, 59, 12358. https://doi.org/10.1016/j.ejrh.2025.102358
- Li, X., & Xiao, J. (2019). Mapping photosynthesis solely from solar-induced chlorophyll fluorescence: A global, fine-resolution dataset of gross primary production derived from OCO-2. *Remote Sensing*, 11(21), 2563. https://doi.org/10.3390/rs11212563
- Lian, X., Piao, S., Li, L. X., Li, Y., Huntingford, C., Ciais, P., et al. (2020). Summer soil drying exacerbated by earlier spring greening of northern vegetation. *Science Advances*, 6(1), eaax0255. https://doi.org/10.1126/sciadv.aax0255
- Light, B., Smith, M. M., Perovich, D. K., Webster, M. A., Holland, M. M., Linhardt, F., et al. (2022). Arctic sea ice albedo: Spectral composition, spatial heterogeneity, and temporal evolution observed during the mosaic drift. *Elementa: Science of the Anthropocene*, 10(1), 000103. https://doi.org/10.1525/elementa.2021.000103
- Maslanik, J., & Stroeve, J. (2004). DMSP SSM/I-SSMIS daily polar gridded brightness temperatures, version 4 [Dataset]. NASA National Snow and Ice Data Center Distributed Active Archive Center. https://doi.org/10.5067/AN9A18EO7PX0
- Milly, P. C. D., & Dunne, K. A. (2020). Colorado River flow dwindles as warming-driven loss of reflective snow energizes evaporation. *Science*, 367(6483), 1252–1255. https://doi.org/10.1126/science.aay9187
- Mioduszewski, J. R., Rennermalm, A. K., Robinson, D. A., & Wang, L. (2015). Controls on spatial and temporal variability in northern hemisphere terrestrial snow melt timing, 1979–2012. *Journal of Climate*, 28(6), 2136–2153. https://doi.org/10.1175/JCLI-D-14-00558.1
- Munné-Bosch, S., & Alegre, L. (2004). Die and let live: Leaf senescence contributes to plant survival under drought stress. *Funtion Plant Biology*, 31(3), 203–216. https://doi.org/10.1071/FP03236
- Muñoz-Sabater, J. (2019). Era5-land monthly averaged data from 1950 to present [Dataset]. Copernicus Climate Change Service (C3S) Climate Data Store (CDS). https://doi.org/10.24381/cds.68d2bb30
- Muñoz-Sabater, J., Dutra, E., Agustí-Panareda, A., Albergel, C., Arduini, G., Balsamo, G., et al. (2021). ERA5-Land: A state-of-the-art global reanalysis dataset for land applications. *Earth System Science Data*, 13(9), 4349–4383. https://doi.org/10.5194/essd-13-4349-2021
- O'Leary, D. S., Hall, D. K., Digirolamo, N. E., & Riggs, G. A. (2020). Regional trends in snowmelt timing for the Western United States throughout the MODIS era. *Physical Geography*, 8, 1–23, https://doi.org/10.1080/02723646.2020.1854418
- Ono, K., Nishi, Y., Watanabe, A., & Terashima, I. (2001). Possible mechanisms of adaptive leaf senescence. *Plant Biology*, 3(3), 234–243. https://doi.org/10.1055/s-2001-15201
- O'Toole, D., Brandt, L. A., Janowiak, M. K., Schmitt, K. M., Shannon, P. D., Leopold, P. R., et al. (2019). Climate change adaptation strategies and approaches for outdoor recreation. Sustainability, 11(24), 7030. https://doi.org/10.3390/su11247030
- Pausas, J. G., & Keeley, J. E. (2021). Wildfires and global change. Frontiers in Ecology and the Environment, 19(7), 387–395. https://doi.org/10.1002/fee.2359
- Pirk, N., Aalstad, K., Yilmaz, Y. A., Vatne, A., Popp, A. L., Horvath, P., et al. (2023). Snow-vegetation-atmosphere interactions in alpine tundra. Biogeosciences, 20(11), 2031–2047. https://doi.org/10.5194/bg-20-2031-2023
- Prbstl-Haider, U., Hdl, C., Ginner, K., & Borgwardt, F. (2021). Climate change: Impacts on outdoor activities in the summer and shoulder seasons. Journal of Outdoor Recreation and Tourism, 34, 100344. https://doi.org/10.1016/j.jort.2020.100344
- Qie, X., Qie, K., Wei, L., Zhu, K., Sun, Z., Yuan, S., et al. (2022). Significantly increased lightning activity over the Tibetan Plateau and its relation to thunderstorm genesis. *Geophysical Research Letters*, 49(16), e2022GL099894. https://doi.org/10.1029/2022GL099894
- Qin, Y., Xiao, X., Dong, J., Zhang, Y., Wu, X., Shimabukuro, Y., et al. (2019). Improved estimates of forest cover and loss in the Brazilian Amazon in 2000–2017. Nature Sustainability, 2(8), 764–772. https://doi.org/10.1038/s41893-019-0336-9
- Rantanen, M., Karpechko, A. Y., Lipponen, A., Nordling, K., Hyvärinen, O., Ruosteenoja, K., et al. (2022). The arctic has warmed nearly four times faster than the globe since 1979. Communications Earth and Environment, 3(1), 168. https://doi.org/10.1038/s43247-022-00498-3
- Riihel, K. K. A. M. L. W., Anttila, K., Manninen, T., Luojus, K., Wang, L., & Riihelä, A. (2019). Intercomparison of snow melt onset date estimates from optical and microwave satellite instruments over the northern hemisphere for the period 1982–2015. *Journal of Geophysical Research: Atmospheres*, 124(21), 11205–11219. https://doi.org/10.1029/2018JD030197
- Scholten, R. C., Coumou, D., Luo, F., & Veraverbeke, S. (2022). Early snowmelt and polar jet dynamics co-influence recent extreme Siberian fire seasons. *Science*, 378(6623), 1005–1009. https://doi.org/10.1126/science.abn4419
- Semain, G. (2015). Principles and practice of structural equation modeling (4th ed.). (methodology in the social sciences) paperback november 12, 2015.

XU ET AL. 15 of 16

23284277, 2025, 10, Downlo.

- Seneviratne, S. I., Corti, T., Davin, E. L., Hirschi, M., Jaeger, E. B., Lehner, I., et al. (2010). Investigating soil moisture-climate interactions in a changing climate: A review. *Earth-Science Reviews*, 99(3–4), 125–161. https://doi.org/10.1016/j.earscirev.2010.02.004
- Shao, D., Li, H., Wang, J., Hao, X., Che, T., & Ji, W. (2022). Reconstruction of a daily gridded snow water equivalent product for the land region above 45° n based on a ridge regression machine learning approach. Earth System Science Data, 14(2), 795–809. https://doi.org/10.5194/essd-14-795-2022
- Slatyer, R. A., Umbers, K. D. L., & Arnold, P. A. (2021). Ecological responses to variation in seasonal snow cover. *Conservation Biology*, 36(1), e13727. https://doi.org/10.1111/cobi.13727
- Takala, M., Pulliainen, J., Metsamaki, S. J., & Koskinen, J. T. (2009). Detection of snowmelt using spaceborne microwave radiometer data in Eurasia from 1979 to 2007. IEEE Transactions on Geoscience and Remote Sensing, 47(9), 2996–3007. https://doi.org/10.1109/TGRS.2009. 2018442
- Trabucco, A., & Zomer, R. (2019). Global aridity index and potential evapotranspiration (et0) database: Version 3 [Dataset]. https://doi.org/10.6084/m9.figshare.7504448.v5
- Vavrus, S. (2007). The role of terrestrial snow cover in the climate system. Climate Dynamics, 29(1), 73–88. https://doi.org/10.1007/s00382-007-0226-0
- Vrese, P. D., Stacke, T., Rugenstein, J. C., Goodman, J., & Brovkin, V. (2021). Snowfall-albedo feedbacks could have led to deglaciation of snowball Earth starting from mid-latitudes. *Communications Earth and Environment*, 2(1), 91. Article number: 91. https://doi.org/10.1038/ s43247-021-00160-4
- Wang, L., Derksen, C., Brown, R., & Markus, T. (2013). Recent changes in pan-arctic melt onset from satellite passive microwave measurements. Geophysical Research Letters, 40(3), 522–528, https://doi.org/10.1002/grl.50098
- Wang, L., Toose, P., Brown, R., & Derksen, C. (2016). Frequency and distribution of winter melt events from passive microwave satellite data in the pan-arctic, 1988–2013. *The Cryosphere*, 10(6), 2589–2602. https://doi.org/10.5194/tc-10-2589-2016
- Westerling, A. L., Hidalgo, H. G., Cayan, D. R., & Swetnam, T. W. (2006). Warming and earlier spring increase Western U.S. forest wildfire activity. *Science*, 313(5789), 940–943. https://doi.org/10.1126/science.1128834
- Xiao, M. (2021). A warning of earlier snowmelt. Nature Climate Change, 11(5), 1-2. https://doi.org/10.1038/s41558-021-01024-7
- Yao, Y., Liu, Y., Zhou, S., Song, J., & Fu, B. (2023). Soil moisture determines the recovery time of ecosystems from drought. Global Change Biology, 29(13), 3562–3574. https://doi.org/10.1111/gcb.16620
- Zheng, B., & Bentler, P. M. (2024). Enhancing model fit evaluation in SEM: Practical tips for optimizing chi-square tests. Structural Equation Modeling: A Multidisciplinary Journal, 32, 1–6. https://doi.org/10.1080/10705511.2024.2354802
- Zheng, B., Ciais, P., Chevallier, F., Hui, Y., Canadell, J. G., Chen, Y., et al. (2023). Record-high CO<sub>2</sub> emissions from boreal fires in 2021. *Science*, 379(6635), 912–915. https://doi.org/10.1126/science.ade0805
- Zheng, B., Ciais, P., Frederic, C., Chuvieco, E., Chen, Y., & Ya, H. (2021). Increasing forest fire emissions despite the decline in global burned area. *Science Advances*, 7(39), eabh2646. https://doi.org/10.1126/sciadv.abh2646
- Zheng, J., Jia, G., & Xu, X. (2022). Earlier snowmelt predominates advanced spring vegetation greenup in Alaska. Agricultural and Forest Meteorology, 315, 108828. https://doi.org/10.1016/j.agrformet.2022.108828
- Zheng, L., Cheng, X., Chen, Z., Wang, S., Liang, Q., & Wang, K. (2022). Global snowmelt onset reflects climate variability: Insights from spaceborne radiometer observations. *Journal of Climate*, 35(10), 2945–2959. https://doi.org/10.1175/JCLI-D-21-0265.1
- Zomer, R. J., Xu, J., & Trabucco, A. (2022). Version 3 of the global aridity index and potential evapotranspiration database. *Scientific Data*, 9(1), 409. https://doi.org/10.1038/s41597-022-01493-1
- Zona, D., Lafleur, P. M., Hufkens, K., Bailey, B., Gioli, B., Burba, G., et al. (2022). Earlier snowmelt May lead to late season declines in plant productivity and carbon sequestration in arctic tundra ecosystems. *Scientific Reports*, 12(1), 3986. Article number: 3986. https://doi.org/10.1038/s41598-022-07561-1

XU ET AL. 16 of 16